CFD Study of Quadcopter Aerodynamics at Static Thrust Conditions

Conference Paper · April 2018

CITATIONS
0

READS
2,662

2 authors:

Erdem Yilmaz
University of Bridgeport
1 PUBLICATION **0** CITATIONS
SEE PROFILE

Junling Hu
University of Bridgeport
79 PUBLICATIONS **918** CITATIONS
SEE PROFILE

CFD Study of Quadcopter Aerodynamics at Static Thrust Conditions

Erdem Yilmaz, Junling Hu
Department of Mechanical Engineering, School of Engineering
University of Bridgeport

***Abstract* – Drone propellers are rotating wings producing lift in the direction of the axis of rotation. Propeller blade design is critical to generate enough thrust to carry the takeoff weight and reduce aerodynamics noise level. In this project, numerical analysis is conducted for the aerodynamics performance of two propeller designs at the static thrust condition. The first design is based on the original DJI Spark drone propeller blade and the second design add a winglet to the first design. 3D CAD models were created in SOLIDWORKS and were imported to SimScale, a cloud-based software, for the computational fluid dynamics (CFD) analysis. The winglet propeller was found to generate 21% more thrust than the original propeller without winglets. The flow patterns, including pressure and velocity distributions were compared for both propeller models.**

***Index Terms* - Aero-acoustic, Computational fluid dynamics (CFD), Drone, Noise measurement, Quadcopter, SolidWorks, SIMSCALE**

I. INTRODUCTION

In recent years, unmanned aerial vehicles (UAVs) has received attention from both academia and industry for their ability to be utilized in numerous applications from film making, logistics, and mining to military purposes. As a result of growing interest in UAVs, the development of multi-rotor UAVs, also referred to as drones, has dramatically accelerated due to its capability of vertical take-off and landing, improved surveillance resolution, and the ease of preparation. With the-state-of-the-art technology in the size and the resolution of cameras, companies, such as DJI, have improved high-quality camera integrated drones in a variety of sizes, fly-times, and camera qualities. These drones have been launched to the market for both recreational and non-recreational drone users, which expanded the use of drones to residential areas. Despite the fact that the small size of such drones can be considered more appealing to users, the noise produced by drones is becoming a concern as it discomforts the users, residents, and even animals nearby. Accordingly, drone manufacturers are putting more effort to the design of propellers to reduce noise in addition to increase the thrust of the propellers.

With this aim, a variety of studies within the field of UAV have been published in the literature. In this regard, Leslie et al.[1] proposed a study on broadband noise in UAV propellers aimed at proving the major source of noise produced by a propeller is a laminar separation bubble which occurs on propeller due to low Reynolds number conditions existing on blades. As a result of this study, they acknowledged that the noise of the drone can be decreased by changing the shape, diameter or angular velocity of the propeller. Moreover, Panagiotou et al. [2] proposed a study on a winglet optimization procedure for a Medium-Altitude-Long-Endurance (MALE) UAV, which aimed at optimizing induced drag caused by the pressure imbalance at the tip of the wing. This study focused on the comparable results through six wing configurations. As a result, a 10% increase in flight time is achieved. Similarly, Turanoğuz and Alemdaroğlu [3] presented a study on designing and improving aerodynamic performance of a UAV by using different winglet designs, where the authors investigated to target reduction in power required to take off the drone by increasing the lift-drag ratio. With regards to this method, they used four different configurations of wingtip geometry to accomplish the comparable results through blended type wingtip design to improve in efficiency and performance of the given aircraft.

Additionally, Gill and D'Andrea [4] examined a methodology for modelling the thrust, drag, and torque of propellers used in the UAV applications for hover and high-speed forward flight regimes. Following this method, the propeller model was created using Blade Element Theory (BET) and Blade Element Momentum Theory (BEMT). This study described standard static thrust model of a propeller of a drone when used in forward flight. To this end, they found that induced drag has not occurred on the blade element except at the very tip of the propeller blade. Hence, they suggested an improvement over the hover model which is commonly known for high-speed condition.

Despite the fact that few studies have been presented in the literature regarding the noise effects of propellers. The most relevant research is studied by Intaratep et al. [5], where they tested the performance and noise generated from four different propellers on DJI Phantom II model drone. The configurations of the propellers were based on the material with no significant differences in design of the blades. This study resulted in the signs of laminar boundary layer vortex shedding noise at some rotational speeds. Furthermore, the thrust produced by a propeller was related to the blade geometry and rotor configuration.

To the best of our knowledge, our study is a novel research which focuses on the noise effect of propellers in the consideration of propeller design. With this motivation, we aim at designing a propeller with a new wingtip design in order improve lift-drag ratio and thrust value, thus the propeller will

perform better under the same conditions with lower angular velocity, which will result in lower noise level.

The details of the proposed methodology and a numerical example along with some comparisons are elaborated in the following sections.

II. PROPELLER DESIGN

Drone propellers are designed to generate enough trust to carry the takeoff weight and maintain a good lift to drag ratio. The propeller design parameters include blade number, diameter, section geometry, and pitch angle. Two propeller models are created in SOLIDWORKS 2017 for CFD simulations of propeller aerodynamics. The first model followed the specifications of DJI Spark's original propellers as shown in Fig. 1.

Fig. 1. Original propeller

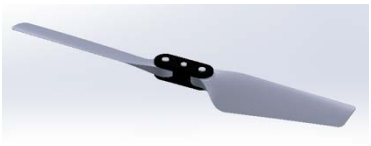

Fig. 2. 3D model of Original propeller

The first 3D CAD model is shown in Fig. 2. The wider side of the blade is twisted by 23°, and the tip is twisted by 15°. The distance from the center of the hole to the tip of the blade is 53.5 mm. The thickness distribution on the body is depicted in Fig. 3.

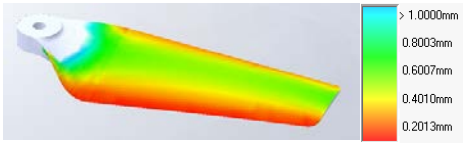

Fig. 3. Thickness distribution on 3D model of Original propeller

Based on the studies [2-4] the tip of the blade has an effect on the lift-drag ratio which can be reduced by a wingtip device. Therefore, a new propeller design with winglet is created by adding a winglet, as shown in Figure 4. The blade is bended by 25° with an additional twist by 2° at the wide side. The distance from center of the hole to the very end of the tip is 53.8 mm. The thickness distribution on the body for this simulation is exhibited in Fig. 5.

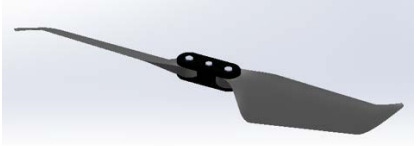

Fig. 4. 3D model of propeller with new design

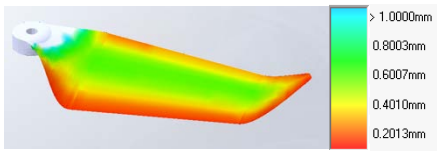

Fig. 5. Thickness distribution on propeller with new design

III. NUMERICAL STUDY

A. Computational Domain and Boundary Condition

Numerical calculations were carried out with SIMSCALE CFD simulations. SST k-omega turbulence model is used to model turbulent flow. The computational domain for the air flow around a rotating propeller includes a background box and a rotating zone. The rotating zone is around the rotor with a diameter of 126 mm and is assigned a fixed angular velocity of 12000 RPM. The background box is outside of the rotating zone with a distance of 346 mm from the center of rotation zone to the top, 525 mm distance from the center of rotation the side boundaries and 1012.5 mm to the bottom.

A no-slip wall boundary condition is assumed on the surfaces of blades and other parts integrated to the geometry. A slip wall boundary conditions are chosen as faces of background box. The air properties are listed in Table I.

TABLE I
AIR FLOW PROPERTIES

Properties	Value
Kinematic viscosity (υ)	1.5295e-5 m^2/s
Density (ρ)	1.1965 kg/m^3

The uniform initial conditions are used as shown in Table IV.

TABLE II
INITIAL CONDITIONS

Properties	Value
Pressure	0 Pa
Velocity	0 m/s
Turbulent kinetic energy value	0.00375 m^2/s^2
Specific turbulence dissipation rate	3.375 $1/s$

B. Mesh Refinement and Mesh Convergence Studies

Cartesian box 1 and 2 are generated in order to create finer mesh around the rotating zone. Specifications of Cartesian box 1 and Cartesian box 2 are presented in Table III.

TABLE III
SPECIFICATIONS OF MAIN ZONES (mm)

	x(+)	x(-)	y(+)	y(-)	z(+)	z(-)
Cartesian box-1	180	180	146	300	180	180
Cartesian box-2	100	100	50	100	100	100

Increasing level of mesh refinement is assigned in the four zones of the computational domain, from the background box, Cartesian box-1, Cartesian box-2, to the rotating zone. Surface

mesh refinement is also conducted on the blade surfaces. Layer refinement is also applied resolve the flow details near the blade surface.

Mesh convergence studies were performed on both propeller models with three meshes. The number of nodes and elements for each set of mesh are listed in Table IV. The thrusts found with each set of mesh and their difference relative to the one found with the finest set of mesh are listed in Table V. The computational time required for the highest level of mesh refinement is 22 hours on a 32-processor computer. The results in Table 5 shows that the results differences are within 6% for the original model and less than 1% for the winglet model.

TABLE IV
SPECIFICATIONS OF MESHES GENERATED (mm)

Meshes	Nodes	2D elements	3D elements
Original Blade Mesh No.1	736,835	2,055,433	659,744
Original Blade Mesh No.2	3,560,129	10,136,992	3,291,537
Original Blade Mesh No.3	20,767,676	60,267,595	19,780,976
Blade (Winglet) Mesh No.1	590,683	1,643,870	527,388
Blade (Winglet) Mesh No.2	4,034,392	11,352,311	3,664,355
Blade (Winglet) Mesh No.3	23,270,999	67,527,119	22,130,399

TABLE V
SPECIFICATIONS OF MESHES GENERATED (mm)

Meshes	Thrust (N)	% of Difference
Original Blade Mesh No.1	0.9821	-6%
Original Blade Mesh No.2	0.9805	-6%
Original Blade Mesh No.3	0.9243	-
Blade (Winglet) Mesh No.1	1.20	-0.6%
Blade (Winglet) Mesh No.2	1.1855	0.5%
Blade (Winglet) Mesh No.3	1.1922	-

C. Simulation results

Figs. 6 and 7 show the thrust time history obtained with the finest set of mesh variation for the corresponding original propeller and the propeller with a winglet. Both figures show that the solution have reached the convergence with time.

Figs. 8-11 show the pressure and velocity fields for the original model. The top surface of propeller blade has lower pressure while the bottom surface has higher pressure. The pressure differences at the two surfaces result in a net thrust of 0.9243 N. The cross-sectional view of pressure distributions in the air near the blade surface show the high pressure filed below the blade and low pressure field above the blade. The velocity field in the air also shows the vortex flow below the blade. The main contribution of the trust is near the tip, where has high flow velocity.

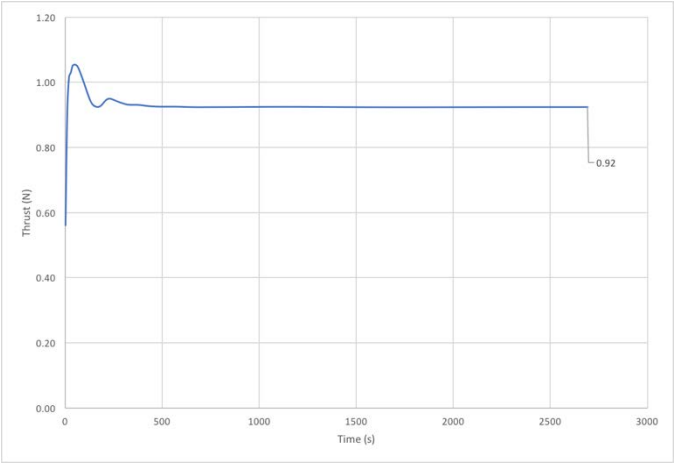

Fig. 6. The thrust variation versus simulation time with fine mesh for the original propeller model

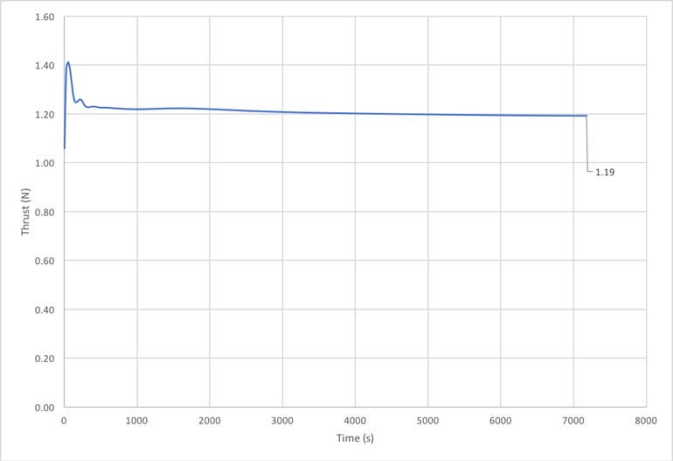

Fig. 7. The thrust variation versus simulation time with fine mesh for the winglet propeller

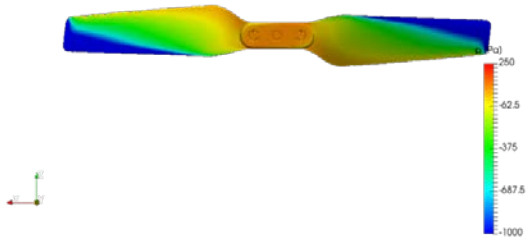

Fig. 8. The pressure distribution at the top surface of the blade for the original propeller

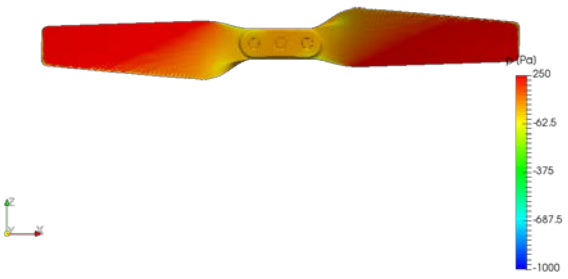

Fig. 9. The pressure distribution at the bottom surface of the blade for the original propeller

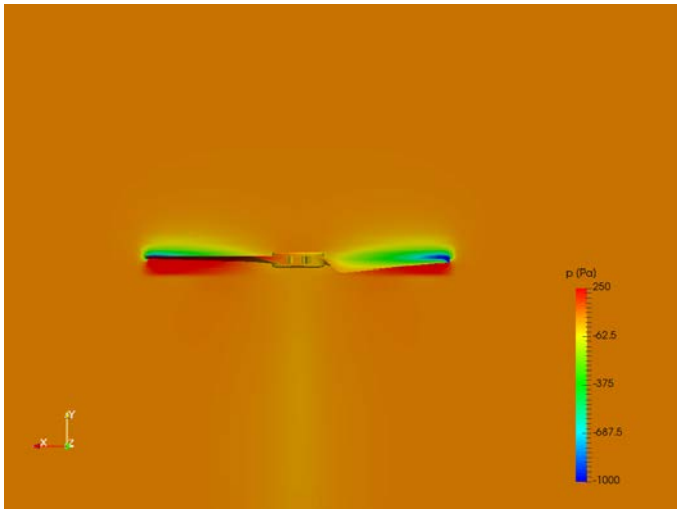

Fig. 10. The pressure distribution in the cross sectional and surface view for the original propeller

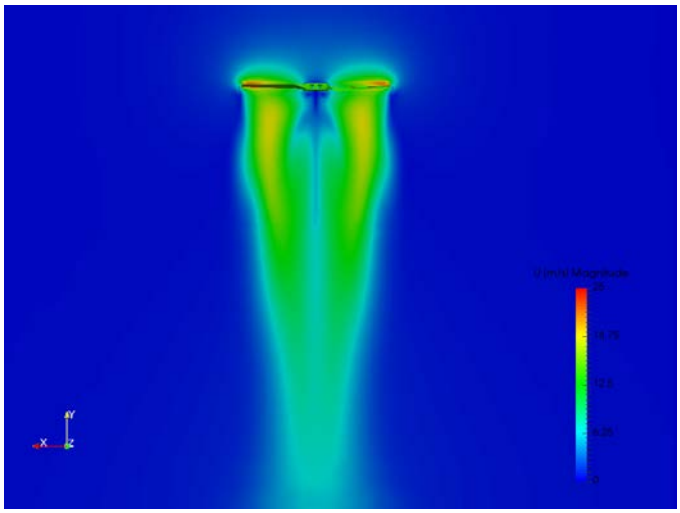

Fig. 11. The velocity contours of the cross sectional and surface view for the original propeller

Figs. 12-15 show the pressure and velocity fields for the winglet model. The similar flow field is observed for the winglet. It is also found that the winglet has extended the high pressure area at the top surface of propeller blade and the low pressure area at the bottom surface area. Therefore, a higher thrust of 1.1922 N is obtained for the winglet model. A more intense vortex flow is observed below the propeller blade compared to the original blade without a winglet.

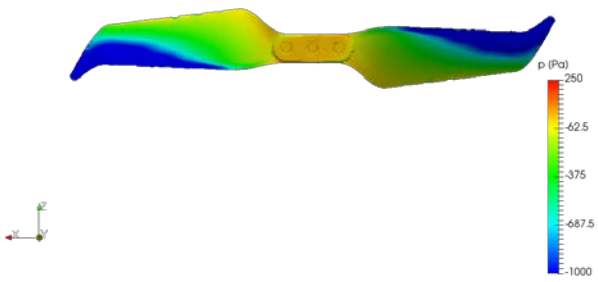

Fig. 12. The pressure distribution at the top surface of the blade for the winglet propeller

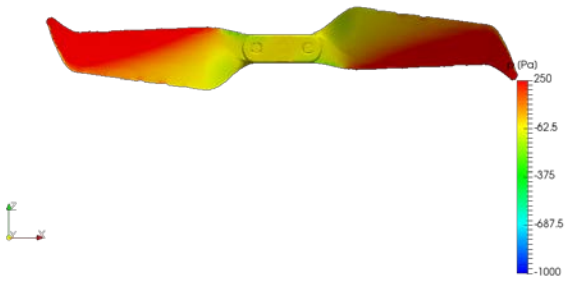

Fig. 13. The pressure distribution at the bottom surface of the blade for the winglet propeller

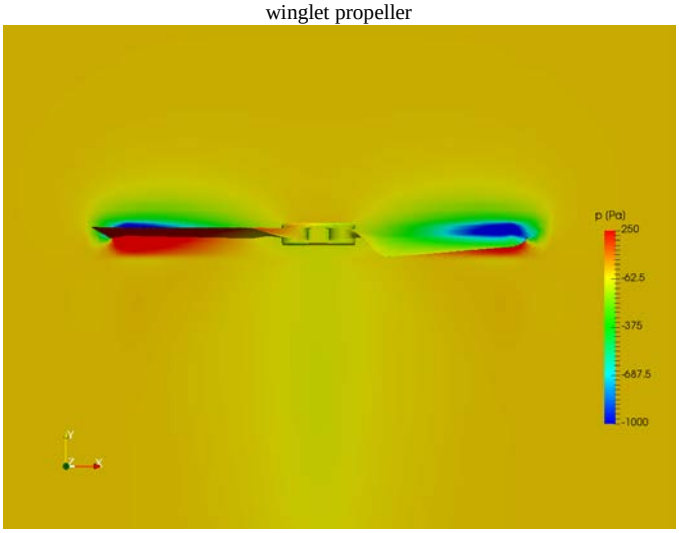

Fig. 14. The pressure contours of the cross sectional and surface view for the winglet propeller

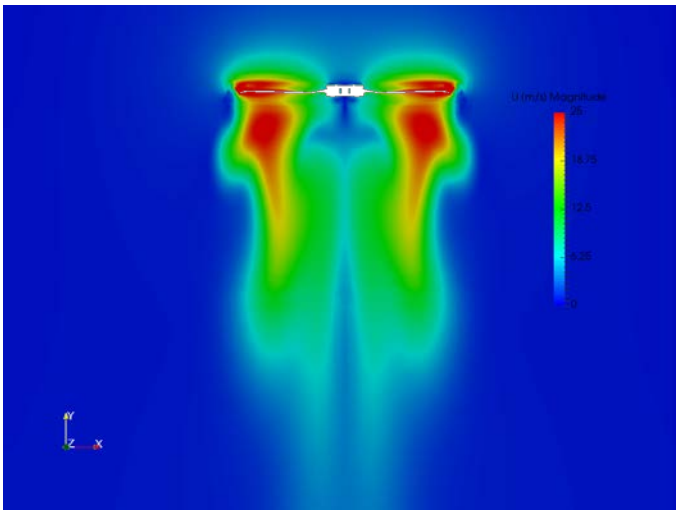

Fig. 15. The velocity contours of the cross sectional and surface view for the original propeller

IV. Conclusion

This paper conducted a numerical analysis of rotor blade at the static thrust condition. Two aerodynamics around two propellers are simulated in SimeScale using the k-omega SST turbulence model. The flow features of the two designs are studied. It was found that the winglet design can increase the thrust by 21% at the same rotational speed. Lower rotational

speed can be used with the winglet propeller in order to reduce noise. Further experimental study will be carried out to measure the thrust to validate with the simulation results and measure the noise level with various propeller blade designs.

REFERENCES

[1] A. Leslie, K. Wong, and D. Auld, "Experimental analysis of the radiated noise from a small propeller," in *Proceedings of 20th International Congress on Acoustics, ICA*, 2010.

[2] P. Panagiotou, P. Kaparos, and K. Yakinthos, "Winglet design and optimization for a MALE UAV using CFD," *Aerospace Science and Technology*, vol. 39, pp. 190-205, 2014.

[3] E. Turanoğuz and N. Alemdaroğlu, "Design of a medium range tactical UAV and improvement of its performance by using winglets," in *Unmanned Aircraft Systems (ICUAS), 2015 International Conference on*, 2015, pp. 1074-1083: IEEE.

[4] R. Gill and R. D'Andrea, "Propeller thrust and drag in forward flight," in *Control Technology and Applications (CCTA), 2017 IEEE Conference on*, 2017, pp. 73-79: IEEE.

[5] N. Intaratep, W. N. Alexander, W. J. Devenport, S. M. Grace, and A. Dropkin, "Experimental study of quadcopter acoustics and performance at static thrust conditions," in *22nd AIAA/CEAS Aeroacoustics Conference*, 2016, p. 2873.